Title	Nonmuscle myosin heavy chain IIA mediates Epstein-Barr virus infection of nasopharyngeal epithelial cells
Author(s)	Xiong, D; Du, YL; Wang, HB; Zhao, B; Zhang, HL; Li, Y; Hu, LJ; Cao, JY; Zhong, Q; Liu, WL; Li, MZ; Zhu, XF; Tsao, GSW; Hutt-Fletcher, LM; Song, E; Zeng, YX; Kieff, E; Zeng, MS
Citation	Proceedings of the National Academy of Sciences, 2015, v. 112 n. 35, p. 11036-11041
Issued Date	2015
URL	http://hdl.handle.net/10722/220049
Rights	Proceedings of the National Academy of Sciences. Copyright © National Academy of Sciences.; This work is licensed under a Creative Commons Attribution-NonCommercial-NoDerivatives 4.0 International License.

Nonmuscle myosin heavy chain IIA mediates Epstein–Barr virus infection of nasopharyngeal epithelial cells

Dan Xiong[a,1], Yong Du[a,1], Hong-Bo Wang[a,1], Bo Zhao[b,1], Hua Zhang[a], Yan Li[a], Li-Juan Hu[a], Jing-Yan Cao[a], Qian Zhong[a], Wan-Li Liu[a], Man-Zhi Li[a], Xiao-Feng Zhu[a], Sai Wah Tsao[c], Lindsey M. Hutt-Fletcher[d], Erwei Song[e], Yi-Xin Zeng[a], Elliott Kieff[b,2], and Mu-Sheng Zeng[a,2]

[a]State Key Laboratory of Oncology in South China, Collaborative Innovation Center for Cancer Medicine, Department of Experimental Research, Sun Yat-Sen University Cancer Center, Guangzhou 510060, People's Republic of China; [b]Department of Medicine and Microbiology and Immunobiology, Brigham and Women's Hospital and Harvard Medical School, Boston, MA 02115; [c]Department of Anatomy and Center for Cancer Research, University of Hong Kong, Hong Kong, Special Administrative Region 999077, People's Republic of China; [d]Health Science Center, Department of Microbiology and Immunology, Louisiana State University, Shreveport, LA 71130; and [e]Guangdong Provincial Key Laboratory of Malignant Tumor Epigenetics and Gene Regulation, Sun Yat-Sen Memorial Hospital, Sun Yat-Sen University, Guangzhou 510120, People's Republic of China

Contributed by Elliott Kieff, July 13, 2015 (sent for review June 2, 2015)

EBV causes B lymphomas and undifferentiated nasopharyngeal carcinoma (NPC). Although the mechanisms by which EBV infects B lymphocytes have been extensively studied, investigation of the mechanisms by which EBV infects nasopharyngeal epithelial cells (NPECs) has only recently been enabled by the successful growth of B lymphoma Mo-MLV insertion region 1 homolog (BMI1)-immortalized NPECs in vitro and the discovery that neuropilin 1 expression positively affects EBV glycoprotein B (gB)-mediated infection and tyrosine kinase activations in enhancing EBV infection of BMI1-immortalized NPECs. We have now found that even though EBV infected NPECs grown as a monolayer at extremely low efficiency (<3%), close to 30% of NPECs grown as sphere-like cells (SLCs) were infected by EBV. We also identified nonmuscle myosin heavy chain IIA (NMHC-IIA) as another NPEC protein important for efficient EBV infection. EBV gH/gL specifically interacted with NMHC-IIA both in vitro and in vivo. NMHC-IIA densely aggregated on the surface of NPEC SLCs and colocalized with EBV. EBV infection of NPEC SLCs was significantly reduced by NMHC-IIA siRNA knock-down. NMHC-IIA antisera also efficiently blocked EBV infection. These data indicate that NMHC-IIA is an important factor for EBV NPEC infection.

Epstein–Barr virus | nasopharyngeal carcinoma | NMHC-IIA | gH/gL | BMI1

EBV is a nearly ubiquitous human γ-herpesvirus that causes B-cell lymphomas and nasopharyngeal carcinoma (NPC), indicative of tropism for both cell types (1–3). Until recently, the molecular mechanisms of EBV infection of B lymphocytes were better understood than the mechanisms of epithelial cell infection (4). EBV attachment to the B-cell membrane is mediated by interactions between EBV glycoprotein 350 (gp350) and complement receptor type 2 (CR2 or CD21) (5) or CD35 (6). EBV gp42 binding to HLA class II triggers EBV fusion with B cells in the presence of EBV glycoprotein B (gB) and gH/gL (7, 8). For epithelial cells, gH/gL and gB are important for EBV infection (4, 9, 10). Epithelial cells lack HLA class II expression; thus, gp42 cannot trigger EBV and cell fusion. Instead, gp42 inversely suppresses the infection (11), and an antibody against gp350 can enhance infections of CD21/CD35-negative epithelial cells (12). The gH/gL heterodimer is required for virus entry (4) and may be involved in binding (13), as well as fusion of EBV (14–17). However, the crystal structure of EBV gH/gL does not show any known fusion domain (18). It is now thought that gH/gL regulates the fusion function of gB (19). Binding of gH/gL to a subset of αv integrins (e.g., $\alpha v\beta_5$, $\alpha v\beta_6$, or $\alpha v\beta_8$) provides the initial trigger for gB-mediated fusion (16, 20, 21). However, E1D1(gH/gL) antibody or CL59(gH) antibody, with a different epitope, can impair epithelial cell infection (20, 22). Thus, multiple gH/gL domains are critical to EBV infection, and gH/gL may interact with proteins in addition to integrins. Direct interaction of EBV gB amino acids 23–431 with neuropilin 1 (NRP1) and its associated tyrosine kinases is critical for EBV infection of nasopharyngeal epithelial cells (NPECs). NRP1 knock-down or EBV pretreatment with soluble NRP1 suppresses EBV NPEC infection, whereas NRP1 overexpression enhances EBV infection (10). Confocal microscopy and experiments with inhibitors of macropinocytosis indicate that EBV enters NPECs through macropinocytosis and not through clathrin-mediated endocytosis (10).

The principal obstacle to identifying factors that may enable more efficient EBV infection of NPECs and better understanding of the role of EBV in NPC is that EBV is remarkably inefficient in infection of primary or B lymphoma Mo-MLV insertion region 1 homolog (BMI1)-immortalized NPECs. As a polycomb complex protein, BMI1 is a proto-oncogene. BMI1 has an important role in regulating proliferation, senescence, and self-renewal of stem cells (23, 24). BMI1 overexpression immortalizes human epithelial cells and mouse embryonic fibroblasts (25, 26). By optimizing the growth of BMI1-immortalized NPEC cultures, we found

Significance

EBV causes nasopharyngeal carcinoma (NPC), an endemic disease in southern China. Unlike EBV infection of B lymphocytes, the molecular mechanisms and outcomes of EBV infection of epithelial cells are poorly understood. In vitro, EBV infects B lymphoma Mo-MLV insertion region 1 homolog (BMI1)-immortalized nasopharyngeal epithelial cells (NPECs) poorly. We have now established a protocol to infect sphere-like cells derived from monolayer NPECs with EBV. Using this model system, we identified nonmuscle myosin heavy chain IIA (NMHC-IIA) as an important host factor to mediate EBV infection of NPECs. NMHC-IIA knock-down substantially decreased NPEC EBV infection. This improved EBV infection model is likely to enable new insights into the mechanisms of EBV epithelia cell infection and will be useful for the understanding EBV's role and effects in conversion of NPECs to NPC.

Author contributions: E.K. and M.-S.Z. designed research; D.X., Y.D., H.-B.W., H.Z., Y.L., L.-J.H., J.-Y.C., Q.Z., W.-L.L., and M.-Z.L. performed research; X.-F.Z., S.W.T., L.M.H.-F., E.S., and Y.-X.Z. contributed new reagents/analytic tools; Y.L., L.-J.H., and M.-Z.L. cultured the NPECs; J.-Y.C. established the high-infection model; Q.Z. and W.-L.L. assisted with cell culture; and D.X., Y.D., B.Z., L.M.H.-F., E.K., and M.-S.Z. wrote the paper.

The authors declare no conflict of interest.

[1]D.X., Y.D., H.-B.W., and B.Z. contributed equally to this work.

[2]To whom correspondence may be addressed. Email: ekieff@rics.bwh.harvard.edu or zengmsh@mail.sysu.edu.cn.

This article contains supporting information online at www.pnas.org/lookup/suppl/doi:10.1073/pnas.1513359112/-/DCSupplemental.

that BMI1-immortalized NPECs seeded at a 10-fold higher density than used in previous protocols and grew initially as a monolayer. "Spherical cells" then grew above the monolayer. Surprisingly, the spherical cells consistently supported an EBV infection efficiency of ~20–30%, using an estimated EBV multiplicity of infection (MOI) of 300. Using this more efficient in vitro EBV infection protocol, we identified an interaction between nonmuscle myosin heavy chain IIA (NMHC-IIA) and gH/gL on the cell surface, which was critical for more efficient EBV NPEC infection.

Results

Establishment of an Efficient in Vitro EBV Infection Model for BMI1-Immortalized NPECs. We screened primary NPECs, BMI1-immortalized NPECs, and NPC cell lines for susceptibility to cell-free EBV infection. Consistent with previous reports, relatively higher infection efficiencies could only be achieved using very high EBV MOIs: i.e., ~2,500–10,000 per cell (10). BMI1-immortalized NPECs seeded at higher densities than previously formed dense monolayers with sphere-like cells (SLCs) growing above the confluent NPEC monolayer cells (MLCs) (Fig. 1*A*, white arrowheads). Most importantly, SLCs were much more efficiently infected by cell-free recombinant EBV expressing eGFP (EBV-eGFP) at an MOI of ~300, whereas MLCs under usual culture conditions were sparsely infected (Fig. 1*A*). SLCs made by seeding 5×10^5 NPEC/BMI1 cells in 48 wells for 36 h were ~10-fold more highly infected than under previous culture conditions. In subsequent experiments, SLCs formed routinely by seeding 5×10^5 NPEC/BMI1 cells in 48-well plates. The infection efficiency of SLCs from NPEC1-BMI1 or NPEC2-BMI1 cells reached 28.4% and 28.0%, respectively, whereas eGFP-positive cells were only 1.4% and 2.6% in monolayer cultured NPEC1-BMI1 and NPEC2-BMI1 cells at an MOI of about 300 (Fig. 1*B*). The low infection efficiency of monolayer cultured cells by cell-free EBV is similar to a previous report (9). Moreover, the mean fluorescence intensities (MFIs) of EBV-infected SLCs from NPEC1-BMI1 and NPEC2-BMI1 cells were increased by ~39-fold and ~28-fold relative to MLCs (Fig. 1*B*).

To determine if CD21 and CD35 are involved in NPEC/BMI1 EBV infection, we evaluated CD21 and CD35 mRNA expression by quantitative RT-PCR (qRT-PCR) and found none in SLCs (Fig. S1*A*). Thus, high SLC infection rates were not mediated by CD21 or CD35. To screen for other glycoproteins that might mediate SLC infection, we used an antibody-blocking assay, which showed that antibodies against gH/gL (CL59) or gH (E1D1) efficiently blocked SLC EBV infection, whereas 72A1 antibody to gp350 enhanced epithelial cell infection (Fig. 1*C* and Fig. S1 *B* and *C*). These results are consistent with previous observations (12, 13) indicating that EBV gH and gL are critical for EBV NPEC infection.

NMHC-IIA Interacts with gH/gL. To identify gH/gL interacting proteins other than integrins, a myc-tagged gH/gL pull-down was subjected to liquid chromatography-tandem MS (MS/MS) proteomic analysis. EBV-infected SLC lysates were immunoprecipitated with myc-tagged gH/gL. A protein of ~250 kDa (Fig. 2*A*) was pulled down and identified by liquid chromatography-MS/MS as NMHC-IIA (Fig. 2*B*). To verify the association of EBV gH/gL with NMHC-IIA, co-immune precipitation assays were done in HEK 293T cells transfected with FLAG-tagged gH/gL or control plasmids. Immune precipitation with an anti-FLAG antibody identified an association of gH/gL with endogenous NMHC-IIA in HEK 293T cells, whereas a control did not associate with NMHC-IIA (Fig. 2*C*). Further, GST pull-down assays revealed that a NMHC-IIA C-terminal amino acid 1,665–1,960 GST fusion protein bound directly to purified myc-tagged gH/gL (Fig. 2*D*), whereas GST alone did not. These data indicate that gH/gL interacts with NMHC-IIA in vivo and in vitro.

NMHC-IIA Is Located on SLC Membranes and Interacts with gH/gL. NMHC-IIA mainly localized to the cell cytoplasm. HSV-1 infection redistributes NMHC-IIA to the cell membrane (27). We examined NMHC-IIA distribution in MLC and SLC cytoplasmic or cell membrane fractions. NMHC-IIA was mostly in the MLC cytoplasmic fraction, and only a minimum amount was in the membrane fraction (Fig. 3*A*), consistent with previous reports (28). In contrast, NMHC-IIA protein was very abundant in SLC membrane fractions (Fig. 3*A*). To further examine whether gH/gL was associated with NMHC-IIA in the membrane fraction, myc-tagged gH/gL was immunoprecipitated from SLC or MLC membrane fractions and blotted for NMHC-IIA. Myc-tagged gH/gL brought down NMHC-IIA from SLC membrane fractions but not from MLC membrane fractions (Fig. 3*B*). Immunofluorescent staining found NMHC-IIA aggregated on the SLC surface, whereas only weak staining was observed on the neighboring MLC surface. In Triton X-100–treated cells, NMHC-IIA was very abundant in the cytoplasm of MLCs surrounding the SLCs (Fig. 3*C*). We also evaluated the colocalization of EBV and NMHC-IIA on SLC

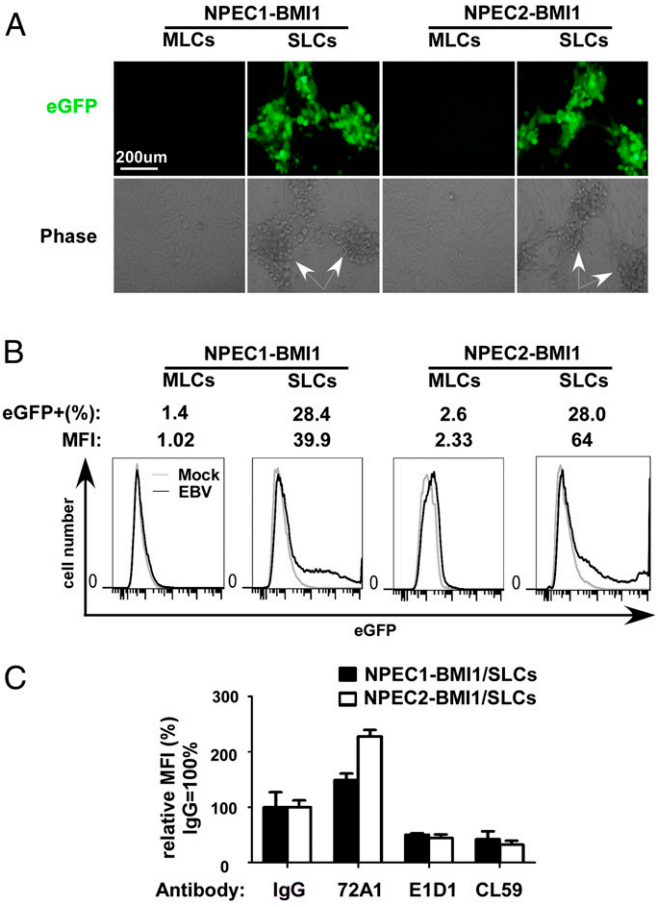

Fig. 1. High-efficiency EBV infection using BMI1-immortalized NPECs. (*A*) NPEC1 or NPEC2 BMI1 cells were seeded at 5×10^4 or 5×10^5 into 48 well plates for 36 h. Cells at 5×10^4 density grew as confluent MLCs, whereas cells at 5×10^5 density formed two layers, with SLCs (white arrowheads indicated) above MLCs. SLCs were more susceptible to EBV infection, whereas MLCs were more resistant to infection. EGFP-positive cells were indicative of successful infection. (*B*) Percentages and MFIs of infected MLCs and SLCs after exposure to EBV-eGFP were analyzed by flow cytometry. The percentages and MFIs of the infected cells were quantified and are labeled above the histogram graph. Gray lines show mock infection, and black lines show EBV-eGFP infection. (*C*) SLCs originated from NPEC1 or NPEC2 BMI1 cells and were exposed to EBV-eGFP after pretreatment with 100 μg/mL mouse IgG, 72A1 (antibody to gp350), E1D1 (antibody to gH/gL), and CL59 (antibody to gH) at 4 °C for 1 h. The infected cell MFIs were measured by flow cytometry 24 h after infection. The mean value of the control IgG was normalized to 100% relative MFI. The error bars are ±SEM.

MICROBIOLOGY

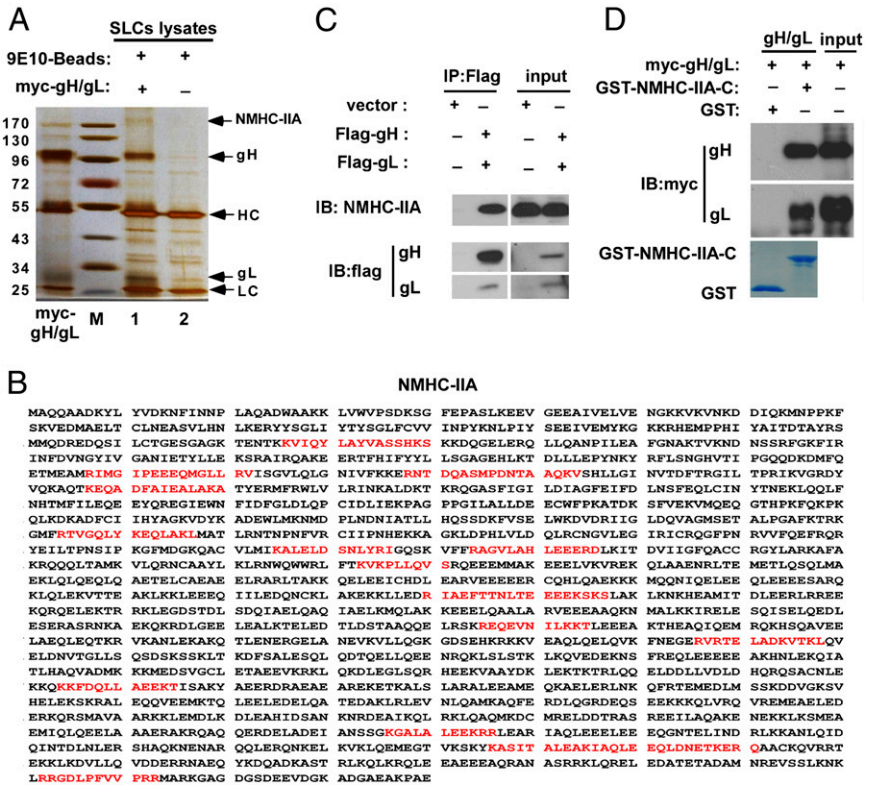

Fig. 2. NMHC-IIA interacts with gH/gL. (*A*) Precipitation of the SLC lysates with myc-gH/gL (lane 1) and BSA (lane 2). The precipitates were separated by SDS/PAGE and subjected to silver staining, and myc-gH/gL was used as a control to exclude false-positive bands. The black arrows indicate the gH/gL, IgG heavy chain (HC), IgG light chain (LC), and a protein differentially pulled down by gH/gL above 170 kDa. (*B*) Sequence coverage (red) for the NMHC-IIA from liquid chromatography-MS analyses of the excised differential band in *A*. (*C*) Lysates of 293T cells transfected with pcep2 vector, pcep2-FLAG-gH/gL, were precipitated with FLAG-M2-antibody and FLAG-gH/gL, and endogenous NMHC-IIA was blotted with FLAG-M2 and NMHC-IIA antibodies, respectively. IB, immunoblot. (*D*) Equivalent amounts of soluble GST and GST-NMHC-IIA-C (amino acids 1,665–1,960) proteins were precipitated with the purified soluble myc-gH/gL. The precipitates were blotted with a myc-antibody. Coomassie blue staining showed equivalent input protein levels in each assay.

membrane. After coculture of EBV and SLCs, antibodies against gp350 and NMHC-IIA were used to visualize EBV and NMHC-IIA using confocal microscopy. We found extensive colocalization of gp350 and NMHC-IIA in NPEC1-BMI1 SLC membranes (Fig. 3*D*). These results indicate that SLC formation caused NMHC-IIA to localize to the cell membrane, and thereby increased EBV SLC infection.

Endogenous NMHC-IIA Inhibition Reduces EBV Binding and SLC Infection. To evaluate the role of endogenous NMHC-IIA in EBV infection of NPEC/BMI1 cells, siRNA knock-down and blocking assays were done. Two siRNAs that target NMHC-IIA were used to reduce NMHC-IIA mRNA and protein expression in NPEC/BMI1 SLCs (Fig. 4*A* and Fig. S2*A*). The siRNAs targeting NMHC-IIA significantly reduced SLC NMHC-IIA expression compared with a negative control siRNA. Decreased membrane NMHC-IIA expression was also evident by immunofluorescence staining in the absence of permeabilization (Fig. S2 *B* and *C*). NPEC/BMI1 SLCs with reduced NMHC-IIA were then infected with EBV-eGFP. Flow cytometry was used to evaluate eGFP expression following EBV infection. NMHC-IIA siRNA knock-down in NPEC1-BMI1 and NPEC2-BMI1 SLCs significantly reduced eGFP signals compared with control siRNA treatment (Fig. 4*B*). Furthermore NMHC-IIA knock-down did not affect adenovirus infection (Fig. 4*B*), consistent with an EBV-specific effect. qRT-PCR was also used to quantify EBV DNA after EBV infection of NPEC1-BMI1 SLCs with reduced NMHC-IIA expression. EBV was incubated with NPEC/BMI1 SLCs expressing reduced NMHC-IIA at 4 °C for 2 h. NMHC-IIA siRNA knock-down significantly (60–82%) reduced EBV copy number compared with control siRNA knock-down (Fig. 4*C*). An antibody-blocking assay was used to further confirm the role of NMHC-IIA in EBV infection. Preincubation of SLCs with a polyclonal NMHC-IIA antibody at 30, 60, or 150 μg/mL inhibited EBV infection in a dose-dependent manner. Antibody blockage at 150 μg/mL reduced MFI by 63% and 72% in NPEC1-BMI1– and NPEC2-BMI1–originated SLCs, respectively (Fig. 4*D*). In contrast, the NMHC-IIA antibody had no effect on adenovirus infection (Fig. 4*D*). Collectively, these results indicate that endogenous NMHC-IIA has a significant role in EBV infection of NPECs.

Expression of NMHC-IIA in Dysplastic Epithelial Cell Membranes. We also evaluated NMHC-IIA expression in normal and dysplastic epithelial cells by immune histochemistry (IHC). NMHC-IIA was highly expressed in the cytoplasm and cell membrane in two of three Epstein–Barr virus-encoded small RNAs (EBERs)-positive dysplastic epithelial tissues (Fig. S3 *A* and *C*). However, NMHC-IIA expression was low in all 12 normal epithelium controls (Fig. S3*B*), and EBERs were not detected in normal epithelium (Fig. S3*D*).

Discussion

This study describes an improved and more efficient NPEC EBV infection model. Using this model, NMHC-IIA was identified as an EBV gH/gL interactive cell protein that has an important role in mediating NPEC EBV infection. Previous studies highlighted two other methods that improved the efficacy of EBV epithelial infection: B-cell transfer infection and cell-free EBV infection. B-cell transfer is a process in which a B cell producing EBV, or

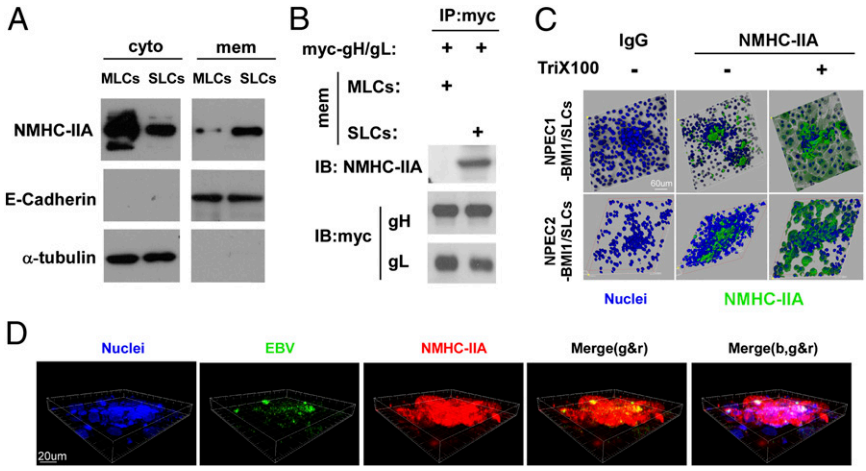

Fig. 3. NMHC-IIA located on the SLC membrane. (*A*) Membrane or its associated MLC and SLC proteins were cross-linked with 3,3′-dithiobis(sulfosuccinimidyl propionate) (DTSSP) and extracted with the ProteoExtract Native Membrane Protein Extraction Kit. The presence of α-tubulin and E-cadherin indicated the cytoplasm and membrane fractions, respectively. The presence of NMHC-IIA was measured in the MLC and SLC cytoplasm and membrane fractions. cyto, cytoplasm fraction; mem, membrane fraction. (*B*) MLC and SLC membrane proteins were immunoprecipitated with purified myc-gH/gL, and the immunoprecipitates (IP) were blotted with NMHC-IIA and myc tag antibodies. (*C*) Typical 3D immunostaining image of NMHC-IIA localization in a field after SLC formation. The cells were incubated with the NMHC-IIA antibody or control IgG, followed by an AF488-conjugated secondary antibody with or without permeabilization by 0.1% Triton X-100 (TriX100) treatment. The nuclei were stained with DAPI (blue). (*D*) Typical 3D immunostaining image of a sphere surface for visualizing the colonization of EBV and NMHC-IIA. NPEC1-BMI1 SLCs were exposed to cell-free EBV-eGFP at 4 °C for 2 h. Then, the unbound EBV was removed by washing with prechilled PBS three times. EBV and NMHC-IIA on the surface of the SLCs were stained with 72A1 (green) and NMHC-IIA (red) antibodies without permeabilization. The nuclei were stained with DAPI (blue). b, blue, g, green, r, red.

having EBV bound to its surface, transfers EBV to an epithelial cell receptor (9, 29–31). Various epithelial cell lines have been evaluated for direct EBV infection. However, EBV transfer infection was not efficient at low MOIs (31). An improvement in EBV infection efficiency was obtained by ectopically expressing CD21 in epithelial cells (32). In the absence of increased CD21 or CD35 expression, we consistently found that EBV infection efficiencies could reach 10–20% when NPEC1-BMI1 cell lines were

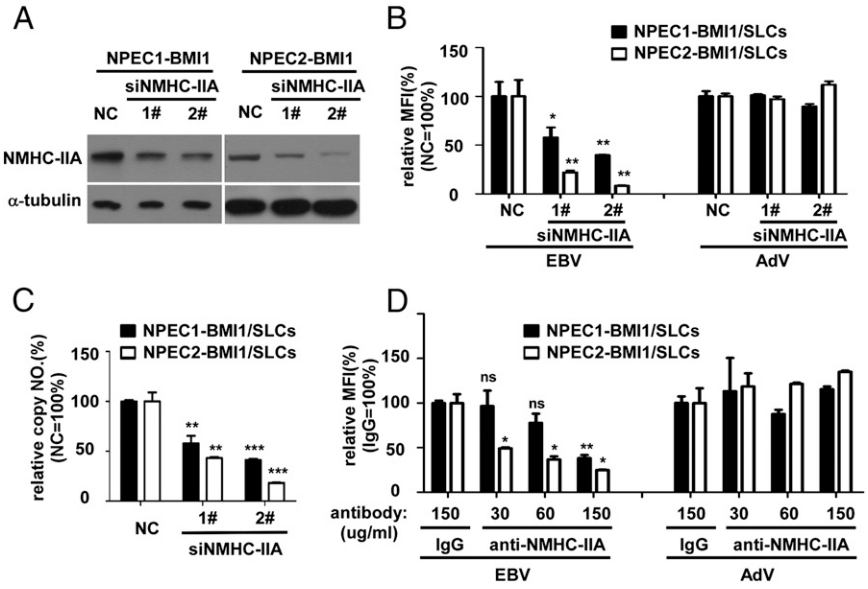

Fig. 4. Inhibition of endogenous NMHC-IIA reduced EBV infection of the SLCs. (*A*) Protein expression levels of NMHC-IIA were determined by immunoblotting 48 h after siRNA transfection. (*B*) Twenty-four hours after transfection, the siRNA-treated cells were reseeded into 48 well plates to form the SLCs. The SLCs were exposed to EBV-eGFP or AdV-eGFP at an MOI of 300 and 10, respectively. Then, the infected cell MFIs were determined 24 h postinfection by flow cytometry. The data are shown as mean and SEM ($n = 3$; two-tailed Student's t test). The mean value of the negative control (NC)-treated SLCs was normalized to 100% relative MFI. The error bars are ±SEM. $*P < 0.05$; $**P < 0.01$. (*C*) EBV copy number on the NMHC-IIA siRNA-treated SLCs was detected with a Taqman probe-based qRT-PCR method. $**P < 0.01$; $***P < 0.001$. (*D*) MLCs and SLCs of the BMI1-immortalized NPECs were pretreated with the indicated concentrations of polyclonal NMHC-IIA antibody or IgG for 1 h at 4 °C. Then, they were exposed to EBV-eGFP or AdV-eGFP at an MOI of 300 and 10, respectively. The infected cell MFIs were determined 24 h after infection by flow cytometry. The data are shown as mean and SEM ($n = 3$). The mean value in the presence of the indicated IgG concentration was normalized to 100% relative MFI. The data are shown as mean and SEM ($n = 3$; two-tailed Student's t test). The error bars are ±SEM. ns, not significant. $*P < 0.05$; $**P < 0.01$.

exposed to high MOIs, such as 2,500–10,000 (10). We have now found that non–CD21-converted, BMI1-immortalized NPEC epithelial cells can be infected with cell-free EBV at a high efficiency and with a relatively low EBV MOI of 300 per cell. Although EBV has not been readily detected in normal nasopharyngeal epithelia, EBV is readily detected in dysplastic nasopharyngeal epithelia and poorly differentiated NPC cells (33). Primary nasopharyngeal epithelial infection may occur in epithelial cells at different stages of development. In precancerous stages, normal nasopharyngeal epithelia, composed of simple columnar or pseudostratified columnar epithelial cells, become disrupted or dysplastic (33) (Fig. S3). Stratified epithelia have been readily infected in an in vitro model (34). BMI1-immortalized NPECs used in these studies had high telomerase activity and reduced p16 expression (25, 26), which are common molecular changes in precancerous nasopharyngeal epithelia (33, 35). SLCs formed from BMI1-immortalized cells may be a model for dysplastic epithelia or precancerous lesions.

EBV gH/gL heterodimers have been reported to bind (13) and fuse (14, 15, 20) to epithelial cells. Integrins $\alpha_5\beta_1$, $\alpha v\beta_5$, $\alpha v\beta_6$, and $\alpha v\beta_8$ are important for EBV infection of epithelial cells (9, 16, 20). Interactions of gH/gL with integrins may trigger virus envelope and cell membrane fusions (16). We have now found that NMHC-IIA is also important for EBV infection of epithelial cells. Although NMHC-IIA is mainly located in the cell cytoplasm, it is also an HSV-1 entry receptor that can be recruited to membranes when HSV-1 attaches to a cell (27). EBV and HSV-1 are evolutionarily related, but also divergent, human herpes viruses that appear to use similar strategies to infect target cells. We found that aggregated NMHC-IIA in apical surfaces of SLCs and NMHC-IIA–enriched membranes likely contribute to high EBV SLC infection efficiency.

NMHC-IIA is highly expressed in the cytoplasm and in dysplastic epithelial cell membranes by IHC staining (Fig. S3*A*). NMHC-IIA expression correlated with EBV infection of dysplastic epithelium, as detected by EBER probes (Fig. S3*C*). NMHC-IIA was expressed at relatively low levels (Fig. S3*B*), however, and EBERs were not detected in normal epithelium (Fig. S3*D*). Because EBV infection did not alter NMHC-IIA expression (Fig. S4), our finding indicates that cells with high levels of NMHC-IIA are more permissive to EBV infection.

NMHC-IIA overexpression in the cytoplasm, without an increase in membrane fraction, did not promote higher EBV infection. Similarly, constitutively high cytoplasmic NMHC-IIA expression had limited effects on EBV infection efficiencies. Higher EBV infection only occurs when NMHC-IIA is redistributed to the cell membrane. The mechanisms through which NMHC-IIA is redistributed to the cell membrane are still not clear. Our data are consistent with a model in which EBV gH/gL interactions with NMHC-IIA and integrins promote efficient EBV entry to epithelial cells. EBV gB and NRP1 are also important for efficient epithelial cell infection (10, 19), where NRP1 facilitates internalization and fusion, as well as macropinocytosis and lipid raft-dependent endocytosis, via direct protein–protein interaction.

The discovery that EBV exploits NMHC-IIA and NRP1 for entry into epithelial cells has important implications for the development of NPC. Inhibitors that can interrupt NMHC-IIA; NRP1; integrins; and EBV gH/gL, gB, or BMRF2 interactions may prevent EBV entry or transformation of NPECs to NPC.

Materials and Methods

Cells, Virus, and Reagents. Primary NPECs and BMI1-immortalized NPECs were grown in keratinocyte serum-free medium (17005-075; Invitrogen). HEK 293T and CHO cells were maintained in DMEM supplemented with 10% (vol/vol) FBS. Akata (EBV-eGFP) and hybridoma cells were grown in RPMI medium 1640 supplemented with 5% (vol/vol) or 10% (vol/vol) FBS, respectively, in humidified 5% (vol/vol) CO_2 incubators at 37 °C. EBV-eGFP cells were made as previously described (36, 37). Briefly, EBV-eGFP cells were produced from Akata (EBV-eGFP) cells by cross-linking cell surface IgG proteins using 0.8% goat anti-human IgG. MLCs and SLCs were exposed to cell-free EBV-eGFP at an MOI of 300 in buffered serum-free RPMI 1640 for 3 h at 37 °C, and excess virus was removed by washing three times with PBS. Antibodies included monoclonal antibodies CL59 to gH (13, 38), E1D1 to gHgL (39), and 72A1 to gp350, obtained from hybridoma (HBM168; American Type Culture Collection) cells. Rabbit IgG was purchased from R&D Systems. Antibody to NMHC-IIA (ab24762) was purchased from Abcam. Rabbit polyclonal antibodies to NMHC-IIA were used to block EBV infection and were produced by immunization with NMHC-IIA (amino acids 1,665–1,960) obtained from Proteintech, with a nonimmunized rabbit IgG used as a control.

Formation of SLCs. A total of 5×10^5 and 5×10^6 BMI1-immortalized NPECs were seeded into 48 well plates and six well plates, respectively. The medium was changed twice daily with preheated keratinocyte serum-free medium to avoid starvation. SLCs formed within 36 h on MLCs.

Determination of Virus Copy Number. To determine the EBV copy number, a TaqMan probe-based qRT-PCR assay was conducted to detect the BamHI-W fragment of the EBV genome (40). A calibration curve was made by detecting the BamHI-W DNA fragment following extraction from Namalwa cells, which contained two integrated viral genomes per cell. The EBV copy number can be calculated in the calibration curve. The estimated MOI of EBV infection is determined by real-time PCR for EBV DNA copy number.

Myc-gH/gL Pull-Down, GST Pull-Down, and Co-Immunoprecipitation Assays. For the Myc-gHgL pull-down assay, lysates from 5×10^7 SLCs were incubated with 9E10 cross-linked agarose beads and 10 μg of myc-gH/gL or 10 μg of BSA in a TNE buffer [50 mM Tris·HCl (pH 7.4), 150 mM NaCl, 0.5% Nonidet P-40, 0.5 mM EDTA, and Roche proteinase inhibitor mixture] for 4 h. The agarose beads were collected following centrifugation and washed four times with TNE buffer. Then, a SDS-buffer solution was added to the agarose beads, and the solution was boiled at 98 °C for 5 min. Next, the proteins that pulled down were separated by SDS/PAGE and subjected to silver staining (P0017S; Beyotime). The soluble myc-gH/gL, myc-tagged gH (amino acids 18–679, lack of intracellular and transmembrane domain), and myc-tagged gL (amino acids 24–137) proteins were expressed and purified in an adenovirus expression system (*SI Materials and Methods*). For co-immunoprecipitation, 293T cells were transfected with pcep2-vector, pcep2-FLAG-gH (amino acids 18–679), or pcep-FLAG-gL (amino acids 24–137). Thirty-six hours later, the cells were lysed in TNE buffer and centrifuged for 10 min at 15,294 × *g*. The supernatants were incubated with FLAG-M2-Beads (Sigma) for 2 h at 4 °C. The immunoprecipitates were collected, washed, and analyzed by immunoblotting with NMHC-IIA antibody. For GST pull-downs, glutathione-Sepharose beads that contained equivalent GST or GST-NMHC-IIA-C [GST-NMHC-IIA (amino acids 1,665–1,960)] levels, which were expressed and purified in *Escherichia coli* BL21 cells (*SI Materials and Methods*), were incubated with myc-gH/gL in TNE buffer overnight at 4 °C. Beads were collected, washed, and analyzed by immunoblotting with a myc antibody.

Membrane Protein Extraction. A total of 5×10^6 BMI1-immortalized NPECs were seeded into six well plates, and 36 h later, the membrane proteins were cross-linked with 3,3′-dithiobis(sulfosuccinimidyl propionate) (DTSSP) (21578; Pierce) at a final concentration of 2 mM in buffered PBS for 2 h on ice. The assay was stopped in 50 mM Tris buffer (pH 7.5) after 15 min. After cross-linking of membrane proteins, SLCs were separated from the MLCs with a time-controlled 0.02% EDTA/PBS treatment and pipetted without destroying the MLCs. The cytoplasm and membrane fractions of the separated SLCs and MLCs were extracted in six well plates according to the ProteoExtract Native Membrane Protein Extraction Kit (catalog no. 444810; Calbiochem) instructions. The extracted cytoplasm and membrane protein concentrations were measured using a QuantiPro BCA Assay Kit (Sigma). Equivalent amounts of MLC and SLC protein were incubated with myc-gH/gL. Immune precipitates were blotted with NMHC-IIA antibody.

Knock-Down Assays. The siRNAs that targeted NMHC-IIA were obtained from Guangzhou RiboBio Co., Ltd., and a total of 2.75×10^5 BMI1-immortalized NPECs were seeded into six well plates. When cell densities reached 80%, cells were transfected with siRNAs using RNAi MAX transfection reagents (Invitrogen), according to the manufacturer's instructions. Twenty-four hours later, 5×10^5 cells were reseeded into 48 well plates to form the SLCs and were subjected to EBV infection after 36 h. The infected cell MFIs were measured by flow cytometry within 24 h postinfection.

Virus Binding Assays. Virus binding assay used a previously published protocol (32). Briefly, virus bound to the cells was harvested after the virus was incubated with cells for 2 h at 4 °C. Then, cells were washed three times with PBS and supplemented with protease inhibitors (Roche) and 15 mg/mL BSA. EBV DNA was isolated using a Blood DNA Kit (Omega), and the relative virus copy number was determined by qRT-PCR (40).

Antibody-Blocking Assay. For antibody-blocking assays, SLCs were pretreated with a polyclonal NMHC-IIA antibody, which was serially diluted to concentrations of 150, 60, and 30 μg/mL in RPMI 1640, or with 150 μg/mL control IgG for 1 h at 4 °C. Cells were then infected with EBV without removing antibody for 3 h at 37 °C. The MFIs of the infected cells were measured within 24 h postinfection by flow cytometry.

FACS Analysis. To detect the percentages and MFIs of EBV-infected cells, cells were trypsinized to a single-cell suspension within 24 h postinfection and were evaluated by flow cytometry (FACS Diva Option; Becton Dickinson).

Immunostaining and Confocal Microscopy. Immunostaining was done using a previously described method (41). Briefly, NMHC-IIA expression levels on MLCs or SLCs were evaluated by indirect immunofluorescence of cells sequentially incubated with a polyclonal rabbit NMHC-IIA antibody (ab24762; Abcam) and AF488/AF594-conjugated anti-rabbit IgG (Life Technology). EBV and NMHC-IIA levels were evaluated using the 72A1 and NMHC-IIA antibodies, respectively, followed by a combined incubation of anti-mouse IgG and anti-rabbit IgG; they were then conjugated with AF488 and AF594, respectively. After washing three times for 5 min, slides were stained with 0.5 μg/mL DAPI (Sigma) to visualize the nuclei and were examined using an Olympus confocal imaging system (Olympus FV1000) with an oil immersion objective with a magnification of 40×. Images were analyzed via Olympus FV 1000 software (Fluoview, version 1.7; Olympus). Each experiment was done in triplicate.

Statistical Analysis. Statistical analyses were performed using the statistical software package SPSS13.0 (IBM). The significance of treatments was determined using the Student's *t* test. *P* values ≤ 0.05 were considered to be statistically significant.

ACKNOWLEDGMENTS. We thank Dr. Maria Masucci (Department of Cell and Molecular Biology, Karolinska Institute) for providing the Akata EBV-eGFP cell line. We thank Dr. Xiaobing Lv (Sun Yat-Sen Memorial Hospital of Sun Yat-Sen University, Guangzhou, People's Republic of China) for providing the adenovirus constructs that contained the EBV glycoprotein genes. This work was supported by the National Basic Research Program of China (Grants 2011CB504300 and 2012CB967003), China National Funds for Distinguished Young Scientists (Grant 81025014), and the National Natural Science Foundation of China (Grant 81202137). This research is also supported by Grant R01CA085180 from the US National Cancer Institute of the United States Public Health Service.

1. Cohen JI (2000) Epstein-Barr virus infection. *N Engl J Med* 343(7):481–492.
2. Lieberman PM (2014) Virology. Epstein-Barr virus turns 50. *Science* 343(6177): 1323–1325.
3. Young LS (2014) Epstein-Barr virus at 50-future perspectives. *Chin J Cancer* 33(11): 527–528.
4. Hutt-Fletcher LM (2007) Epstein-Barr virus entry. *J Virol* 81(15):7825–7832.
5. Tanner J, Weis J, Fearon D, Whang Y, Kieff E (1987) Epstein-Barr virus gp350/220 binding to the B lymphocyte C3d receptor mediates adsorption, capping, and endocytosis. *Cell* 50(2):203–213.
6. Ogembo JG, et al. (2013) Human complement receptor type 1/CD35 is an Epstein-Barr Virus receptor. *Cell Rep* 3(2):371–385.
7. Wang X, Hutt-Fletcher LM (1998) Epstein-Barr virus lacking glycoprotein gp42 can bind to B cells but is not able to infect. *J Virol* 72(1):158–163.
8. Mullen MM, Haan KM, Longnecker R, Jardetzky TS (2002) Structure of the Epstein-Barr virus gp42 protein bound to the MHC class II receptor HLA-DR1. *Mol Cell* 9(2): 375–385.
9. Tugizov SM, Berline JW, Palefsky JM (2003) Epstein-Barr virus infection of polarized tongue and nasopharyngeal epithelial cells. *Nat Med* 9(3):307–314.
10. Wang HB, et al. (2015) Neuropilin 1 is an entry factor that promotes EBV infection of nasopharyngeal epithelial cells. *Nat Commun* 6:6240.
11. Borza CM, Hutt-Fletcher LM (2002) Alternate replication in B cells and epithelial cells switches tropism of Epstein-Barr virus. *Nat Med* 8(6):594–599.
12. Turk SM, Jiang R, Chesnokova LS, Hutt-Fletcher LM (2006) Antibodies to gp350/220 enhance the ability of Epstein-Barr virus to infect epithelial cells. *J Virol* 80(19): 9628–9633.
13. Molesworth SJ, Lake CM, Borza CM, Turk SM, Hutt-Fletcher LM (2000) Epstein-Barr virus gH is essential for penetration of B cells but also plays a role in attachment of virus to epithelial cells. *J Virol* 74(14):6324–6332.
14. Omerović J, Lev L, Longnecker R (2005) The amino terminus of Epstein-Barr virus glycoprotein gH is important for fusion with epithelial and B cells. *J Virol* 79(19): 12408–12415.
15. Wu L, Hutt-Fletcher LM (2007) Point mutations in EBV gH that abrogate or differentially affect B cell and epithelial cell fusion. *Virology* 363(1):148–155.
16. Chesnokova LS, Nishimura SL, Hutt-Fletcher LM (2009) Fusion of epithelial cells by Epstein-Barr virus proteins is triggered by binding of viral glycoproteins gHgL to integrins alphavbeta6 or alphavbeta8. *Proc Natl Acad Sci USA* 106(48):20464–20469.
17. Chen J, Rowe CL, Jardetzky TS, Longnecker R (2012) The KGD motif of Epstein-Barr virus gH/gL is bifunctional, orchestrating infection of B cells and epithelial cells. *MBio* 3(1):e00290–11.
18. Matsuura H, Kirschner AN, Longnecker R, Jardetzky TS (2010) Crystal structure of the Epstein-Barr virus (EBV) glycoprotein H/glycoprotein L (gH/gL) complex. *Proc Natl Acad Sci USA* 107(52):22641–22646.
19. Connolly SA, Jackson JO, Jardetzky TS, Longnecker R (2011) Fusing structure and function: A structural view of the herpesvirus entry machinery. *Nat Rev Microbiol* 9(5): 369–381.
20. Chesnokova LS, Hutt-Fletcher LM (2011) Fusion of Epstein-Barr virus with epithelial cells can be triggered by αvβ5 in addition to αvβ6 and αvβ8, and integrin binding triggers a conformational change in glycoproteins gHgL. *J Virol* 85(24):13214–13223.
21. Chesnokova LS, Ahuja MK, Hutt-Fletcher LM (2014) Epstein-Barr virus glycoprotein gB and gHgL can mediate fusion and entry in trans, and heat can act as a partial surrogate for gHgL and trigger a conformational change in gB. *J Virol* 88(21):12193–12201.
22. Wu L, Borza CM, Hutt-Fletcher LM (2005) Mutations of Epstein-Barr virus gH that are differentially able to support fusion with B cells or epithelial cells. *J Virol* 79(17): 10923–10930.
23. Molofsky AV, He S, Bydon M, Morrison SJ, Pardal R (2005) Bmi-1 promotes neural stem cell self-renewal and neural development but not mouse growth and survival by repressing the p16Ink4a and p19Arf senescence pathways. *Genes Dev* 19(12):1432–1437.
24. Lessard J, Sauvageau G (2003) Bmi-1 determines the proliferative capacity of normal and leukaemic stem cells. *Nature* 423(6937):255–260.
25. Song LB, et al. (2006) Bmi-1 is a novel molecular marker of nasopharyngeal carcinoma progression and immortalizes primary human nasopharyngeal epithelial cells. *Cancer Res* 66(12):6225–6232.
26. Park IK, Morrison SJ, Clarke MF (2004) Bmi1, stem cells, and senescence regulation. *J Clin Invest* 113(2):175–179.
27. Arii J, et al. (2010) Non-muscle myosin IIA is a functional entry receptor for herpes simplex virus-1. *Nature* 467(7317):859–862.
28. Vicente-Manzanares M, Ma X, Adelstein RS, Horwitz AR (2009) Non-muscle myosin II takes centre stage in cell adhesion and migration. *Nat Rev Mol Cell Biol* 10(11): 778–790.
29. Shannon-Lowe C, Rowe M (2011) Epstein-Barr virus infection of polarized epithelial cells via the basolateral surface by memory B cell-mediated transfer infection. *PLoS Pathog* 7(5):e1001338.
30. Shannon-Lowe CD, Neuhierl B, Baldwin G, Rickinson AB, Delecluse HJ (2006) Resting B cells as a transfer vehicle for Epstein-Barr virus infection of epithelial cells. *Proc Natl Acad Sci USA* 103(18):7065–7070.
31. Imai S, Nishikawa J, Takada K (1998) Cell-to-cell contact as an efficient mode of Epstein-Barr virus infection of diverse human epithelial cells. *J Virol* 72(5):4371–4378.
32. Valencia SM, Hutt-Fletcher LM (2012) Important but differential roles for actin in trafficking of Epstein-Barr virus in B cells and epithelial cells. *J Virol* 86(1):2–10.
33. Lo KW, To KF, Huang DP (2004) Focus on nasopharyngeal carcinoma. *Cancer Cell* 5(5): 423–428.
34. Temple RM, et al. (2014) Efficient replication of Epstein-Barr virus in stratified epithelium in vitro. *Proc Natl Acad Sci USA* 111(46):16544–16549.
35. Kong QL, Guan S, Guo BH, Zeng MS (2009) Pre-malignant nasopharyngeal epithelial cell models. *Chin J Cancer* 28(10):1012–1015.
36. Lan K, Verma SC, Murakami M, Bajaj B, Robertson ES (2007) Epstein-Barr Virus (EBV): Infection, propagation, quantitation, and storage. *Curr Protoc Microbiol* Chapter 14: Unit 14E.2.
37. Shimizu N, Yoshiyama H, Takada K (1996) Clonal propagation of Epstein-Barr virus (EBV) recombinants in EBV-negative Akata cells. *J Virol* 70(10):7260–7263.
38. Strnad BC, et al. (1982) Production and characterization of monoclonal antibodies against the Epstein-Barr virus membrane antigen. *J Virol* 41(1):258–264.
39. Li Q, Turk SM, Hutt-Fletcher LM (1995) The Epstein-Barr virus (EBV) BZLF2 gene product associates with the gH and gL homologs of EBV and carries an epitope critical to infection of B cells but not of epithelial cells. *J Virol* 69(7):3987–3994.
40. Lo YM, et al. (1999) Quantitative analysis of cell-free Epstein-Barr virus DNA in plasma of patients with nasopharyngeal carcinoma. *Cancer Res* 59(6):1188–1191.
41. Song LB, et al. (2009) The polycomb group protein Bmi-1 represses the tumor suppressor PTEN and induces epithelial-mesenchymal transition in human nasopharyngeal epithelial cells. *J Clin Invest* 119(12):3626–3636.
42. Weiss LM, Chen YY (2013) EBER in situ hybridization for Epstein-Barr virus. *Methods Mol Biol* 999:223–230.